

Original Research



OPEN ACCESS

Received: Feb 9, 2021

Revised: Mar 31, 2021

Accepted: Apr 27, 2021

Corresponding Authors:

Hyesook Lee

Anti-Aging Research Center, Dong-Eui University, 176 Eomgwang-ro, Busanjin-gu, Busan 47227, Korea.

Tel. +82-51-890-3315

Fax. +82-51-890-3333

E-mail. 14769@deu.ac.kr

Yung Hyun Choi

Department of Biochemistry, Dong-Eui University College of Korean Medicine, 52-57, Yangjeong-ro, Busanjin-gu, Busan 47227, Korea.

Tel. +82-51-890-3319

Fax. +82-51-890-3333

E-mail. choihy@deu.ac.kr


©2021 The Korean Nutrition Society and the Korean Society of Community Nutrition

This is an Open Access article distributed under the terms of the Creative Commons Attribution Non-Commercial License (<https://creativecommons.org/licenses/by-nc/4.0/>) which permits unrestricted non-commercial use, distribution, and reproduction in any medium, provided the original work is properly cited.


ORCID iDs

Hyesook Lee 


<https://orcid.org/0000-0003-3546-9370>

Cheol Park 

<https://orcid.org/0000-0003-4906-0410>

Da Hye Kwon 

<https://orcid.org/0000-0001-5492-7184>

Hyun Hwangbo 

<https://orcid.org/0000-0003-2180-1205>

Schisandrae Fructus ethanol extract attenuates particulate matter 2.5-induced inflammatory and oxidative responses by blocking the activation of the ROS-dependent NF-κB signaling pathway

Hyesook Lee ^{1,2§}, Cheol Park ³, Da Hye Kwon ^{1,2}, Hyun Hwangbo ^{1,2}, So Young Kim ^{1,2}, Min Yeong Kim ^{1,2}, Seon Yeong Ji ^{1,2}, Da Hye Kim ^{1,2}, Jin-Woo Jeong ⁴, Gi-Young Kim ⁵, Hye-Jin Hwang ⁶, and Yung Hyun Choi ^{1,2§}

¹Anti-Aging Research Center, Dong-Eui University, Busan 47340, Korea

²Department of Biochemistry, Dong-Eui University College of Korean Medicine, Busan 47227, Korea

³Division of Basic Sciences, College of Liberal Studies, Dong-Eui University, Busan 47340, Korea

⁴Nakdonggang National Institute of Biological Resources, Sangju 37242, Korea

⁵Department of Marine Life Sciences, Jeju National University, Jeju 63243, Korea


⁶Department of Food and Nutrition, Dong-Eui University, Busan 47340, Korea

ABSTRACT

BACKGROUND/OBJECTIVES: Schisandrae Fructus, the fruit of *Schisandra chinensis* Baill., has traditionally been used as a medicinal herb for the treatment of various diseases, and has proven its various pharmacological effects, including anti-inflammatory and antioxidant activities. In this study, we investigated the inhibitory effect of Schisandrae Fructus ethanol extract (SF) on inflammatory and oxidative stress in particulate matter 2.5 (PM_{2.5})-treated RAW 264.7 macrophages.

MATERIALS/METHODS: To investigate the anti-inflammatory and antioxidant effects of SF in PM_{2.5}-stimulated RAW 264.7 cells, the levels of pro-inflammatory mediator such as nitric oxide (NO) and prostaglandin E₂ (PGE₂), cytokines including interleukin (IL)-6 and IL-1β, and reactive oxygen species (ROS) were measured. To elucidate the mechanism underlying the effect of SF, the expression of genes involved in the generation of inflammatory factors was also investigated. We further evaluated the anti-inflammatory and antioxidant efficacy of SF against PM_{2.5} in the zebrafish model.

RESULTS: The results indicated that SF treatment significantly inhibited the PM_{2.5}-induced release of NO and PGE₂, which was associated with decreased inducible NO synthase and cyclooxygenase-2 expression. SF also attenuated the PM_{2.5}-induced expression of IL-6 and IL-1β, reducing their extracellular secretion. Moreover, SF suppressed the PM_{2.5}-mediated translocation of nuclear factor-kappa B (NF-κB) from the cytosol into nuclei and the degradation of inhibitor IκB-α, indicating that SF exhibited anti-inflammatory effects by inhibiting the NF-κB signaling pathway. In addition, SF abolished PM_{2.5}-induced generation of ROS, similar to the pretreatment of a ROS scavenger, but not by an inhibitor of NF-κB activity. Furthermore, SF showed strong protective effects against NO and ROS production in PM_{2.5}-treated zebrafish larvae.

So Young Kim 
<https://orcid.org/0000-0002-3238-6900>
 Min Yeong Kim 
<https://orcid.org/0000-0001-9083-8218>
 Seon Yeong Ji 
<https://orcid.org/0000-0001-8564-8663>
 Da Hye Kim 
<https://orcid.org/0000-0002-0846-0357>
 Jin-Woo Jeong 
<https://orcid.org/0000-0002-7549-4514>
 Gi-Young Kim 
<http://orcid.org/0000-0002-6878-0790>
 Hye-Jin Hwang 
<http://orcid.org/0000-0002-5448-6443>
 Yung Hyun Choi 
<https://orcid.org/0000-0002-1454-3124>

Funding

This research was funded by the Basic Science Research Program through the National Research Foundation of Korea (grant number: 2019R1C1C1008623).

Conflict of Interest

The authors declare no potential conflicts of interest.

Author Contributions

Conceptualization: Lee H, Park C, Choi YH; Data curation: Kim GY, Hwang HJ, Choi YH; Formal analysis: Park C, Kim DH, Hwangbo H, Kim SY, Kim MY, Ji SY, Kwon DH, Jeong JW; Project administration: Lee H; Investigation: Lee H, Park C, Ji SY, Kim DH, Jeong JW; Methodology: Kwon DH, Hwangbo H, Kim SY, Kim MY; Supervision: Choi YH; Writing - original draft: Lee H, Kim GY, Hwang HJ, Choi YH; Writing - review & editing: Lee H, Choi YH.

CONCLUSIONS: Our findings suggest that SF exerts anti-inflammatory and antioxidant effects against PM2.5 through ROS-dependent down-regulating the NF-κB signaling pathway, and that SF can be a potential functional substance to prevent PM2.5-mediated inflammatory and oxidative damage.

Keywords: Particulate matter; oxidative stress; inflammation; reactive oxygen species; NF-kappa B

INTRODUCTION

In recent years, airborne particulate matter (PM), which is a major component of air pollution, is receiving a lot of attention as a harmful factor to the human body [1,2]. As a result of the great efforts to research the adverse effects of PM on health, many evidences have accumulated that PM causes respiratory disease, cardiovascular disease, skin aging, exacerbation of allergic conditions, various cancers including lung cancer, and other diseases [3-5]. Although PM is defined by its diameter, its chemical composition is considered the most important in determining its biohazard effect. Particularly, PM2.5, which is less than 2.5 μm in diameter, is composed of various heavy metal ions, nitrates, sulfates, carbon substances, as well as harmful viruses and bacteria [6,7]. Recent studies demonstrate that there is a direct association between the inflammatory response and oxidative stress in various cellular dysfunctions caused by PM2.5. For example, in macrophages exposed to PM2.5, the production of pro-inflammatory mediators and cytokines was increased through the activation of nuclear factor-kappa B (NF-κB) [8-10], which was associated with increased neutrophil recruitment and vascular permeability [11,12]. Moreover, previous studies have demonstrated the ability of PM2.5 to produce reactive oxygen species (ROS) and related species, and the resulting oxidative environment of the cells has been reported to lead to cell death following loss of function of organelles within the cell [13-15]. These oxidative stresses may be related to the regulation of intracellular signaling pathways leading to transcription of pro-inflammatory genes [16-18]. Therefore, agents with potent anti-inflammatory and antioxidant properties that are not toxic may be potential candidates for preventing or improving PM-mediated damage.

Recently, many natural products have shown protective effects against a variety of diseases through anti-inflammatory and antioxidant properties. *Schisandra chinensis* (Turcz.) Baill., belonging to the genus Schisandra, is one of the most widely used traditional medicinal plants due to its various therapeutic properties [19,20]. A number of previous studies have shown that *S. chinensis* fruit (Schisandrae Fructus) extract and its ingredients have a variety of beneficial pharmacological effects, including anti-inflammatory, antioxidant, neuroprotective, hepatoprotective, immune regulatory and anti-tumor effects [20-22]. For example, Song *et al.* [23] recently demonstrated that Schisandrae Fructus extract acted as an anti-inflammatory agent in lipopolysaccharide (LPS)-stimulated glia cells through blocking of NF-κB and mitogen-activated protein kinase signaling pathways. We also reported that Schisandrae Fructus extract exhibited anti-inflammatory effects by modulating these signaling pathways in an interleukin (IL)-1β-induced osteoarthritis model [24]. Additionally, Schisandrae Fructus has been reported to inhibit the LPS-induced inflammatory response in macrophages by inhibiting the phosphatidylinositol 3-kinase/Akt signaling pathway as well as NF-κB [25]. Moreover, previous studies have reported that the exogenous addition of Schisandrae Fructus extract or its constituents showed strong cytoprotective and antioxidant

effects against various types of oxidative stress-induced cell damage [26,27]. However, the precise mechanisms for the inhibitory effect by Schisandrae Fructus on PM-induced inflammatory and oxidative responses have not been well studied. Therefore, in this study, we sought to investigate the effect of Schisandrae Fructus ethanol extract (SF) on PM2.5-stimulated RAW 264.7 macrophages and to elucidate the mechanisms involved. We also demonstrated the anti-inflammatory and antioxidant potential of SF in zebrafish.

MATERIALS AND METHODS

Preparation of SF

SF was extracted according to a modified previous method [28]. In brief, the frozen Schisandrae Fructus samples provided by Mungyeong Omija Valley Farming Association Co. (Mungyeong, Korea) were sectioned and homogenized using a grinder prior to extraction with 70% ethanol. After soaking the sample at room temperature (RT) for 48 h, the extract was filtered using filter paper (Whatman No. 3; Sigma-Aldrich Chemical Co., St. Louis, MO, USA) and concentrated using a rotary vacuum evaporator (BÜCHI Labortechnik, Flawil, Switzerland). The extract (SF) was freeze-dried and dissolved in dimethyl sulfoxide (DMSO; Invitrogen-Gibco, Carlsbad, CA, USA) to prepare a stock solution (50 mg/mL), and the SF was diluted to the required concentrations with cell culture medium just before use.

Cell culture and treatment

RAW 264.7 cells were obtained from the Korea Cell Line Bank (Seoul, Korea) and maintained in humidified air at 37°C, and 5% CO₂ in Dulbecco's modified Eagle's medium containing 100 U/mL penicillin and streptomycin, and 10% fetal bovine serum. All materials required for the cell culture were purchased from WelGENE Inc. (Daegu, Korea). The PM2.5 used in this study was a standard diesel particulate matter (SRM 1650b) issued by the National Institute of Standards and Technology (Gaithersburg, MD, USA), and was purchased from Sigma-Aldrich Chemical Co.). A 50 mg/mL stock solution of PM2.5 was prepared in DMSO, and diluted to the appropriate concentration (50 µg/mL) in the culture medium before adding to the cells as previously described [14].

Cell viability assay

The cytotoxicity of SF against RAW 264.7 cells in the presence or absence of PM2.5 was determined using the 3-(4,5-dimethylthiazol-2-yl)-2,5-diphenyltetrazolium bromide (MTT) reduction assay as previously described [29]. In brief, the cells were treated with various concentrations of SF alone or pre-treated with the indicated concentrations of SF for 1 h before 50 µg/mL PM2.5 treatment for 24 h. Then, the medium was removed, and MTT solution (0.5 mg/mL; Sigma-Aldrich Chemical Co.) was dispensed into each well and reacted at 37°C. After 3 h incubation, the supernatant was removed and DMSO was added to dissolve the blue formazan crystals for 10 min. The absorbance per well was quantified at a wavelength of 540 nm using an enzyme-linked immunosorbent assay (ELISA) plate reader (Dynatech Laboratories, Chantilly, VA, USA).

Measurement of nitric oxide (NO), prostaglandin E₂ (PGE₂), and cytokines

RAW 264.7 cells were treated with 200 µg/mL and 400 µg/mL SF for 1 h and then stimulated with 50 µg/mL PM2.5 for 24 h. The NO level in the medium was evaluated by the amount of nitrite measured using the Griess reagent (Sigma-Aldrich Chemical Co.) as previously described [30]. Briefly, 100 µL of the cell-conditioned medium was mixed with the same

amount of Griess reagent for 10 min. The absorbance was measured at 540 nm using an ELISA reader and calculated by comparison to a sodium nitrite (NaNO_2) standard curve. To investigate the PGE_2 and cytokine levels, the culture supernatants were collected and assayed using commercially available ELISA kits (R&D Systems Inc., Minneapolis, MN, USA) according to the instructions from the manufacturer. The absorbance was measured at a wavelength of 450 nm using an ELISA reader as previously described [30].

Protein isolation and Western blot analysis

RAW 264.7 cells were treated with 200 and 400 $\mu\text{g}/\text{mL}$ SF, or pre-treated with 200 and 400 $\mu\text{g}/\text{mL}$ of SF for 1 h before 50 $\mu\text{g}/\text{mL}$ PM2.5 treatment for 24 h. To extract whole proteins, the cells were washed with cold phosphate-buffered saline (PBS) and lysed with lysis buffer as previously described [31]. In parallel, nuclear extraction reagents purchased from Pierce (Rockford, IL, USA) were used to isolate proteins from the nucleus and cytoplasm according to the manufacturer's protocol. The concentration of the isolated protein was measured using the Bio-Rad protein assay kit (Bio-Rad Laboratories, Hercules, CA, USA). Equal amounts of protein were separated by sodium dodecyl sulfate-polyacrylamide gel electrophoresis. Proteins in the gel were subsequently transferred to polyvinylidene difluoride membranes (Schleicher and Schuell GmbH, Keene, NH, USA). The protein-transferred membranes were blocked with non-fat dry milk solution (5%) at RT for 1 h, and then reacted with primary antibodies (**Table 1**) overnight at 4°C. The membranes were washed 3 times for 5 min with Tris-buffered saline (0.1% Tween-20) and then incubated with secondary antibodies for 2 h at RT. The membrane was reacted with an enhanced chemiluminescent solution purchased from Amersham Corp. (Arlington Heights, IL, USA) and then exposed to X-ray film to visualize the corresponding proteins. Secondary antibodies for rabbit immunoglobulin G (IgG, rabbit, 1:1,000, #7074) and mouse IgG (mouse, 1:1,000, sc-516102) were obtained from Cell Signaling Technology (Beverly, MA, USA) and Santa Cruz Biotechnology Inc. (Dallas, TX, USA), respectively.

Reverse transcription-polymerase chain reaction (RT-PCR) assay

For RT-PCR assay, RAW 264.7 cells were treated with 200 $\mu\text{g}/\text{mL}$ and 400 $\mu\text{g}/\text{mL}$ SF for 1 h and then cultured with PM2.5 for 24 h. Total RNA was isolated from the cells using TRIzol reagent (Invitrogen Life Technologies, Carlsbad, CA, USA), following the manufacturer's instructions, and quantified. The isolated total RNA (1 μg) was used to synthesize cDNA using AccuPower[®] RT PreMix (Bioneer, Daejeon, Korea) according to the manufacturer's instructions. The cDNA generated at RT was amplified using the One-Step RT-PCR PreMix Kit with selected primers (iNtRON Biotechnology Inc., Seongnam, Korea). The PCR primers were as follows: inducible NO synthase (iNOS) forward, 5'-ATG TCC GAA GCA AAC ATC AC-3' and reverse, 5'-TAA TGT CCA GGA AGT AGG TG-3'; cyclooxygenase-2 (COX2) forward, 5'-CAG CAA ATC CTT GCT GTT CC-3' and reverse, 5'-TGG GCA AAG AAT GCA AAC ATC-

Table 1. List of antibodies used for western blot analysis in the present study

Antibody	Manufacturer	Item No.	Dilution
iNOS	BD Biosciences (San Jose, CA, USA)	610328	1:1,000
COX-2	Cayman Chemical Company (Ann Arbor, MI, USA)	160126	1:500
IL-6	Santa Cruz Biotechnology, Inc. (Dallas, TX, USA)	sc-28343	1:1,000
IL-1 β	Santa Cruz Biotechnology, Inc. (Dallas, TX, USA)	sc-7884	1:1,000
NF- κB	Santa Cruz Biotechnology, Inc. (Dallas, TX, USA)	sc-8008	1:500
I κB - α	Cell Signaling Technology (Beverly, MA, USA)	#9242	1:500
Laminin B	Santa Cruz Biotechnology, Inc. (Dallas, TX, USA)	sc-374015	1:1,000
Actin	Santa Cruz Biotechnology, Inc. (Dallas, TX, USA)	sc-47778	1:1,000

iNOS, inducible nitric oxide synthase; COX-2, cyclooxygenase-2; IL, interleukin; NF- κB , nuclear factor-kappa B.

3'; IL-6 forward, 5'-GGA GGC TTA ATT ACA CAT GTT-3' and reverse, 5'-TGA TTT CAA GAT GAA TTG GAT-3'; IL-1 β forward, 5'-ATG GCA ACT GTT CCT GAA CTC AAC T-3' and reverse, 5'-TTT CCT TTC TTA GAT ATG GAC AGG AC-3'; and glyceraldehyde-3-phosphate dehydrogenase (GAPDH) forward, 5'-AGG CCG GTG CTG AGT ATG TC-3' and reverse, 5'-TGC CTG CTT CAC CAC CTT CT-3'. The following PCR conditions were applied: GAPDH: 18 cycles of denaturation at 94°C for 30 s, annealing at 57°C for 30 s, and extension at 72°C for 30 s; iNOS, COX-2, IL-6 and IL-1b: 25 cycles of denaturation at 94°C for 30 s, annealing at 52°C for 30 s, and extension at 72°C for 30 s. GAPDH was used as an internal control to evaluate relative expression of COX-2, iNOS, IL-6 and IL-1b. The amplified DNA products were electrophoresed on 1.5% agarose gels and visualized after ethidium bromide (EtBr; Sigma-Aldrich Chemical Co.) staining as previously described [32].

Immunofluorescence for NF- κ B

RAW 264.7 cells were seeded into 4-well cell culture slides and stabilized for 24 h. The cells were pre-treated with 400 μ g/mL SF for 1 h and then treated with or without 50 μ g/mL PM2.5 for 1 h. After treatment, the cells were fixed with ice-cold methanol for 10 min and washed with PBS. Subsequently, the cells were blocked using 5% bovine serum albumin (BSA; Sigma-Aldrich Chemical Co.) with PBS-T (PBS containing 0.1% Triton X) for 1 h and then incubated with anti-NF- κ B (1:100 in 2.5% BSA in PBS-T) at 4°C overnight. The cells were washed with PBS-T and incubated with the secondary antibody (goat anti-rabbit IgG cross-absorbed secondary antibody conjugated to Alexa Fluor 594; Thermo Fisher Scientific, Waltham, MA, USA) for 1 h. After washing with PBS, the cells were counterstained with 4',6-diamidino-2-phenylindole (Sigma-Aldrich Chemical Co.) for 20 min to stain the nuclei. Cell fluorescence was observed using a fluorescence microscope (Carl Zeiss, Oberkochen, Germany) at Core-Facility Center for Tissue Regeneration (Dong-Eui University, Busan, Korea).

Measurement of ROS levels

The levels of ROS production were measured using 5,6-carboxy-2',7'-dichlorofluorescein diacetate (DCF-DA; Sigma-Aldrich Chemical Co.). Briefly, RAW 264.7 cells were pre-treated with 400 μ g/mL SF, 10 mM N-acetyl cysteine (NAC; Sigma-Aldrich Chemical Co.), and/or 20 μ M 4-methyl-N¹-(3-phenyl-propyl)-benzene-1,2-diamine (JSH-23; Sigma-Aldrich Chemical Co.) for 1 h and then incubated for 1 h in the absence or presence of 50 μ g/mL PM2.5. The cells were stained with 10 μ M DCF-DA for 15 min in the dark at 37°C. The cells were then washed with PBS and immediately analyzed by flow cytometry (BD Biosciences, San Jose, CA, USA) as previously described [33]. To compare the degree of ROS generation through fluorescence microscopic observation, the cells were stained with DCF-DA for 15 min at 37°C and then fixed with paraformaldehyde solution (4%, pH 7.4) for 20 min. The cells were washed with PBS and analyzed for ROS fluorescence intensity using a fluorescence microscope.

Zebrafish maintenance and PM2.5 treatment

AB strain zebrafish, which were provided by Dr. Kang CH (Nakdong National Institute of Biological Resources, Sangju, Korea) were maintained at 28.5°C with a 14/10 h light/dark cycle according to the standard guidelines of the Animal Care and Use Committee of Jeju National University (Jeju, Korea; Approval No. 2019-0053). Fertilized embryos were collected after natural spawning as previously described [34] and cultured in 2 mg/L methylene blue containing E3 embryo media at 28.5°C. Three days post-fertilized (dpf) zebrafish larvae were treated with 200 μ g/mL and 400 μ g/mL SF for 1 h and then placed in E3 media containing 0.5 μ g/mL PM2.5 for 24 h.

NO and ROS staining in zebrafish larvae

The production of NO and ROS in zebrafish larvae was visualized using 4-amino-5-methylamino-2'-7'-difluorofluorescein diacetate (DAF-FM-DA; Sigma-Aldrich Chemical Co.) and DCF-DA, respectively, 24 h after treatment as previously described [34]. In brief, zebrafish embryos (4 dpf) were transferred to 24-well plates and incubated with 5 μ M DAF-FM-DA and 20 μ M DCF-DA for 30 min and visualized using the CELENA[®] S Digital Imaging System (Logos Biosystems, Anyang, Korea). Fluorescence intensities were calculated using ImageJ software (Wayne Rasband; National Institute of Health, Bethesda, MD, USA) and expressed as a percentage compared to the untreated control.

Statistical analysis

The data were analyzed with GraphPad Prism software (GraphPad Software, Inc., La Jolla, CA, USA) using one-way analysis of variance for multiple comparisons, followed by Tukey's *post hoc* test. All numerical data are presented as the mean \pm standard deviation of at least triplicate experiments. *P*-values of less than 0.05 were considered statistically significant.

RESULTS

Effect of SF on the proliferation of RAW 264.7 macrophages

The cytotoxic effect of SF on RAW 264.7 cells was determined by the MTT assay. According to the results of this study, at concentrations below 400 μ g/mL SF was not cytotoxic to RAW 264.7 cells. Subsequent experiments showed that the survival rate of RAW 264.7 cells treated with 50 μ g/mL PM2.5 alone was slightly lower than that of control cells, but there was no statistical difference between the 2 groups. Additionally, administration of less than 400 μ g/mL SF to 50 μ g/mL PM2.5-treated RAW 264.7 cells did not show any significant adverse effects on cell viability (data not shown).

SF inhibits PM2.5-induced NO and PGE₂ production in RAW 264.7 macrophages

To evaluate the anti-inflammatory effects of SF, changes in the levels of released pro-inflammatory mediators such as NO and PGE₂ were detected in RAW 264.7 cells pre-treated with SF for 1 h and then stimulated with PM2.5 for 24 h. As shown in **Fig. 1A and B**, PM2.5 treatment greatly increased the release of NO and PGE₂ compared to the untreated control, but this increase was significantly reduced in SF-pre-treated cells in a concentration-dependent manner. Next, we investigated whether SF could inhibit the expression of iNOS and COX-2 by PM2.5. According to the RT-PCR and Western blot results, the mRNA and protein expression of iNOS and COX-2 increased by PM2.5 was significantly suppressed in the presence of SF (**Fig. 2**).

SF reduces the production and expression of PM2.5-induced pro-inflammatory cytokines in RAW 264.7 macrophages

Next, we investigated the effect of SF on the production and expression of pro-inflammatory cytokines increased by PM2.5 treatment. Our results showed that the amount of pro-inflammatory cytokines, including IL-6 and IL-1 β released into the culture supernatant after stimulation with PM2.5 increased significantly. However, the enhanced production of these cytokines by PM2.5 was significantly suppressed by SF pretreatment, and this effect was dependent upon the SF treatment concentration (**Fig. 1C and D**). Subsequently, whether the inhibition of cytokine production by SF in PM2.5-treated RAW 264.7 cells was associated with the decreased expression of these genes was also investigated. As shown in **Fig. 2**,

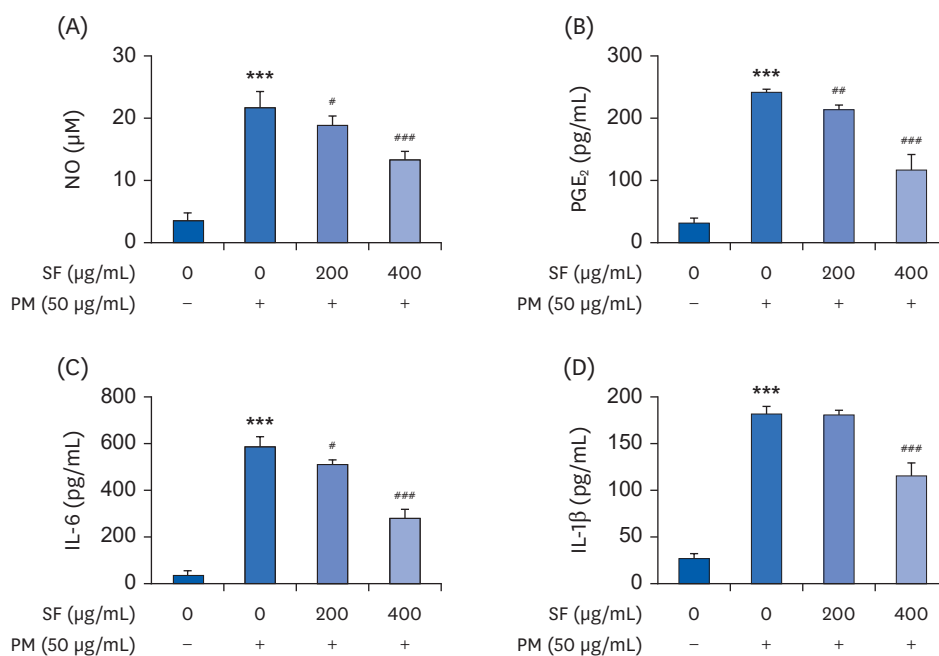


Fig. 1. Effect of SF on the production pro-inflammatory mediators and cytokines in PM2.5-stimulated RAW 264.7 macrophages. Cells were treated with the indicated concentrations of SF for 1 h and then stimulated with 50 µg/mL PM2.5 for 24 h. (A) The NO concentration in the culture medium was determined by the Griess reaction. (B–D) The PGE₂ (B), IL-6 (C), and IL-1β (D) concentration was determined using commercial ELISA kits. The absorbance was measured using a microplate reader. The error bars represent the mean ± SD of 3 independent experiments. SF, Schisandrae Fructus ethanol extract; PM, particulate matter; NO, nitric oxide; PGE₂, prostaglandin E₂; IL, interleukin; ELISA, enzyme-linked immunosorbent assay. ****P* < 0.001 vs. PM2.5-unstimulated cells; **P* < 0.05, ***P* < 0.01 and *****P* < 0.001 vs. PM2.5-stimulated cells.

PM2.5 treatment significantly increased the expression of these cytokine proteins, but their expression was reduced in cells pre-treated with SF.

SF suppresses the nuclear translocation of NF-κB in PM2.5-stimulated RAW 264.7 macrophages

We further investigated whether SF inhibits the PM2.5-mediated activation of NF-κB because it is a key factor controlling the transcription of pro-inflammatory enzymes and cytokines. As shown in **Fig. 3A and B**, when RAW 264.7 cells were stimulated with PM2.5, the expression of NF-κB in the nucleus was significantly increased compared with the control group. By contrast, the level of IκB-α in the cytoplasm was decreased by the treatment of PM2.5, indicating that NF-κB was activated. However, SF reduced the nuclear accumulation of NF-κB p65, and the degradation of IκB-α induced by PM2.5. Consistent with the immunoblotting results, the increase in fluorescence intensity of NF-κB p65 observed in the nuclei of PM2.5-treated cells was markedly decreased by pretreatment with SF, as shown in **Fig. 3C**.

SF alleviates the PM2.5-mediated generation of ROS in RAW 264.7 macrophages

Because oxidative stress also plays an important role in the activation of macrophages and inducing inflammatory responses, we investigated whether SF suppresses PM2.5-induced oxidative stress using the DCF-DA probe. The flow cytometry results showed that the levels of intracellular ROS contents increased with the stimulation of PM2.5 (**Fig. 4A and B**). However, the increase in ROS content in RAW 264.7 cells treated with PM2.5 was dramatically reduced by the addition of SF. In addition, PM2.5-induced ROS production was significantly decreased through NAC pretreatment, a ROS scavenger, but the NF-κB specific inhibitor JSH-

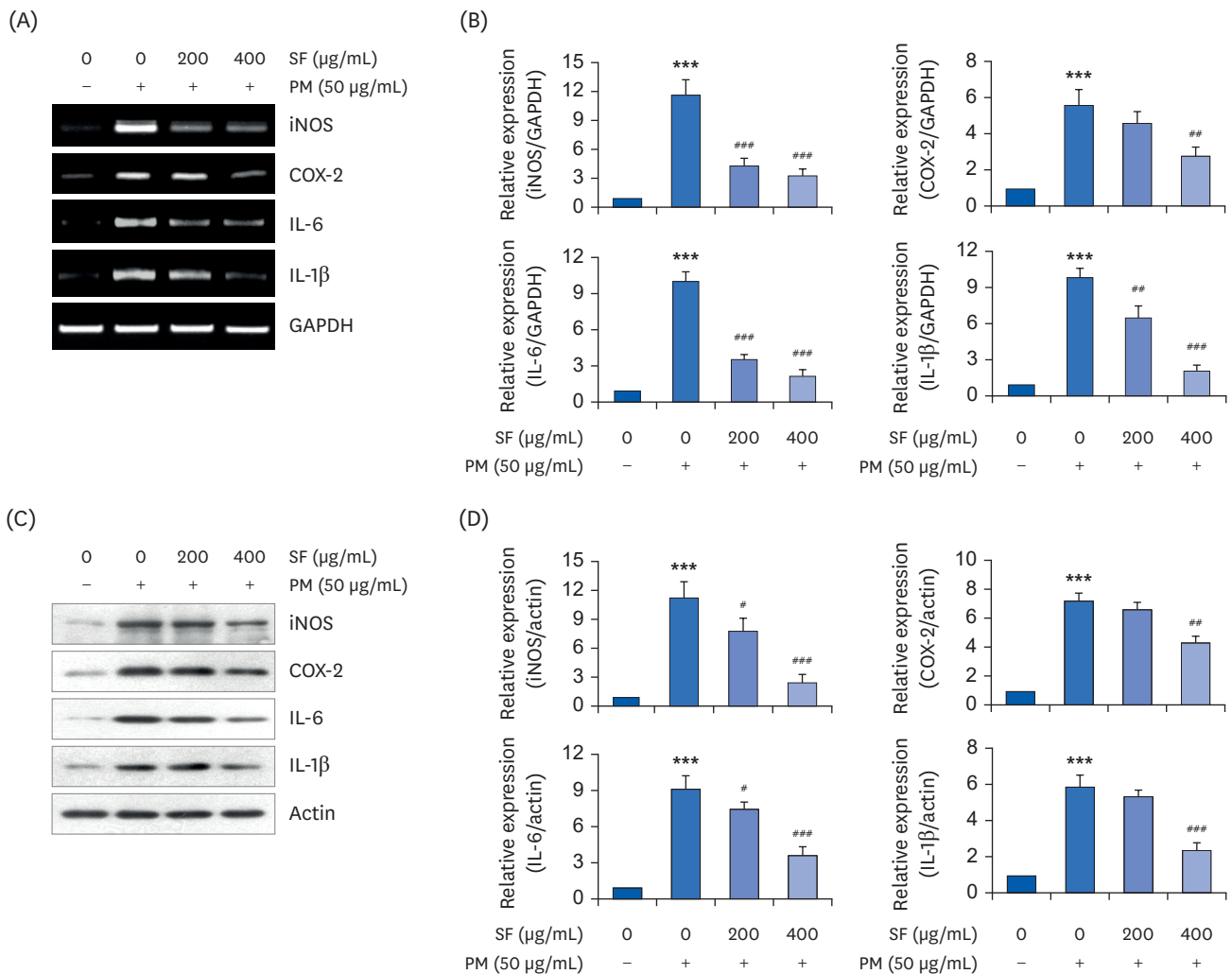


Fig. 2. Effect of SF on the expression of pro-inflammatory enzymes and cytokines in PM2.5-stimulated RAW 264.7 macrophages. Cells were treated with the indicated concentrations of SF for 1 h and then stimulated with 50 μ g/mL PM2.5 for 24 h. After treatment, total RNA and protein were extracted from the cells. The expression levels of iNOS, COX-2, IL-6, and IL-1 β mRNA (A) and proteins (C) were measured by RT-PCR and Western blot analysis, respectively. GAPDH and actin and were used as internal controls for the RT-PCR and Western blot analyses, respectively. (B, D) Bands were quantified using ImageJ and normalized to GAPDH and actin, and the ratio was determined. Data are expressed as the mean \pm SD of 3 independent experiments. SF, Schisandrae Fructus ethanol extract; PM, particulate matter; iNOS, inducible nitric oxide synthase; COX-2, cyclooxygenase-2; IL, interleukin; RT-PCR, reverse transcription-polymerase chain reaction; GAPDH, glyceraldehyde-3-phosphate dehydrogenase. *** P < 0.001 vs. PM-unstimulated cells; * P < 0.05, ** P < 0.01 and **** P < 0.001 vs. PM-stimulated cells.

23 failed to alleviate the redox disorders caused by PM2.5. Consistent with the results from the flow cytometry, the increase in the fluorescence intensity of DCF-DA observed in the cells treated with PM2.5 was weakened by pretreatment of SF (Fig. 4C).

The inhibitory effect of SF on PM2.5-induced NF- κ B activation and inflammatory response is ROS-dependent in RAW 264.7 macrophages

We next investigated whether the inhibitory effect of SF on NF- κ B activation and inflammatory response in PM2.5-treated cells was ROS-dependent. As shown in Fig. 5A and B, PM2.5-induced nuclear accumulation of NF- κ B p65 and degradation of I κ B- α were markedly inhibited in the presence of NAC. Furthermore, the increased production of inflammatory mediator and cytokine such as NO and IL-6 by PM2.5 was significantly canceled under the condition of NAC pretreatment, similar to that in SF pre-treated cells (Fig. 5C and D).

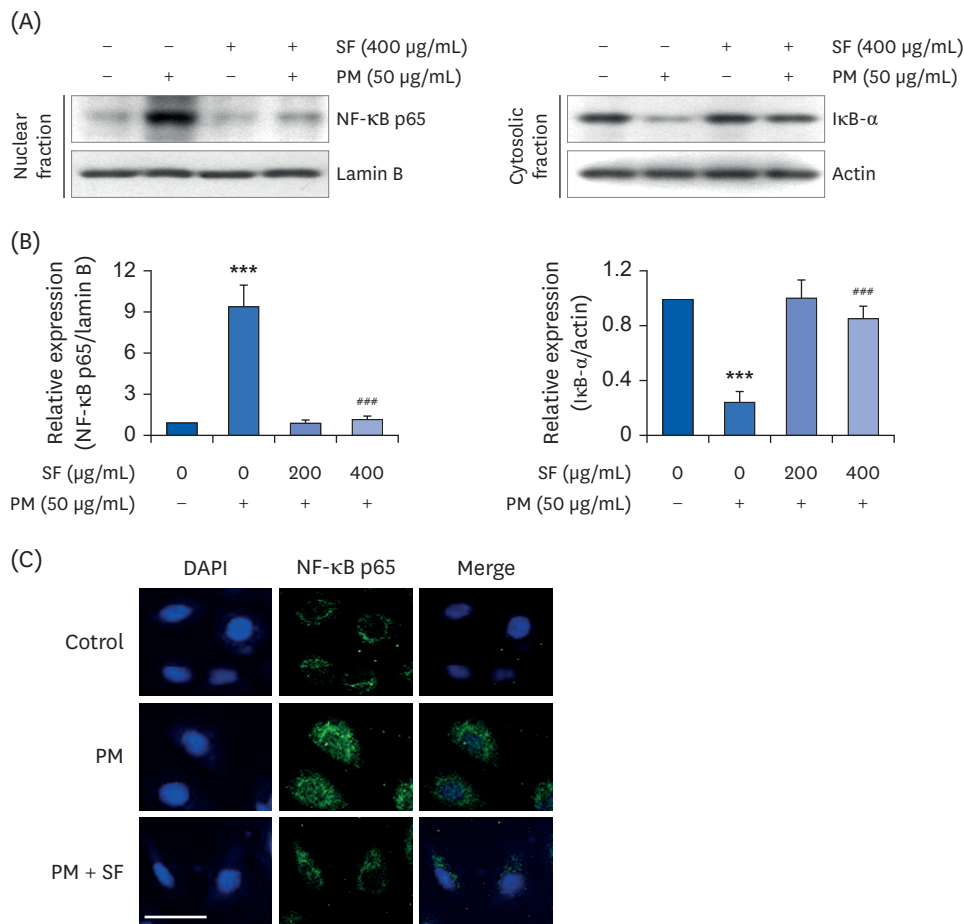


Fig. 3. Inactivation of NF-κB signaling pathway by SF in PM2.5-stimulated RAW 264.7 macrophages. Cells were treated with 400 μg/mL SF alone for 24 h or pre-treated with or without 400 μg/mL SF for 1 h before 50 μg/mL PM2.5 stimulation for 1 h. (A) For Western blot analysis, nuclear and cytosolic proteins were isolated, and the expression of NF-κB and IκB-α was investigated. Protein loading was confirmed by the analysis of lamin B or actin expression in each protein extract. (B) Bands were quantified using ImageJ and normalized to lamin B and actin, and the ratio was determined. Data are expressed as the mean ± SD of 3 independent experiments. (C) The cells were subjected to immunofluorescence staining with NF-κB p65 antibody and representative fluorescence images were acquired using a fluorescence microscope. Green fluorescence indicates the localization of NF-κB p65 and blue fluorescence by DAPI staining allows visualization of the nuclei (scale bar = 200 μM).

SF, Schisandrae Fructus ethanol extract; PM, particulate matter; NF-κB, nuclear factor-kappa B; DAPI, 4',6-diamidino-2-phenylindole.

*** $P < 0.001$ vs. PM-unstimulated cells; ### $P < 0.001$ vs. PM-stimulated cells.

SF weakens the production of NO and ROS in PM2.5-treated zebrafish larvae

As SF downregulates inflammatory and oxidative responses in RAW 264.7 macrophages, we wondered if SF had a similar effect in the *in vivo* model and demonstrated it using the zebrafish model. According to the results of DAF-FM-DA staining, PM2.5 treatment significantly increased NO generation. However, in the presence of SF within a non-toxic range, the PM2.5-induced NO generation gradually decreased in a concentration-dependent manner (Fig. 6A and B). In addition, we confirmed by DCF-DA staining that the increased ROS accumulation in PM2.5-stimulated zebrafish larvae was dose-dependently abrogated in the presence of SF (Fig. 6C and D).

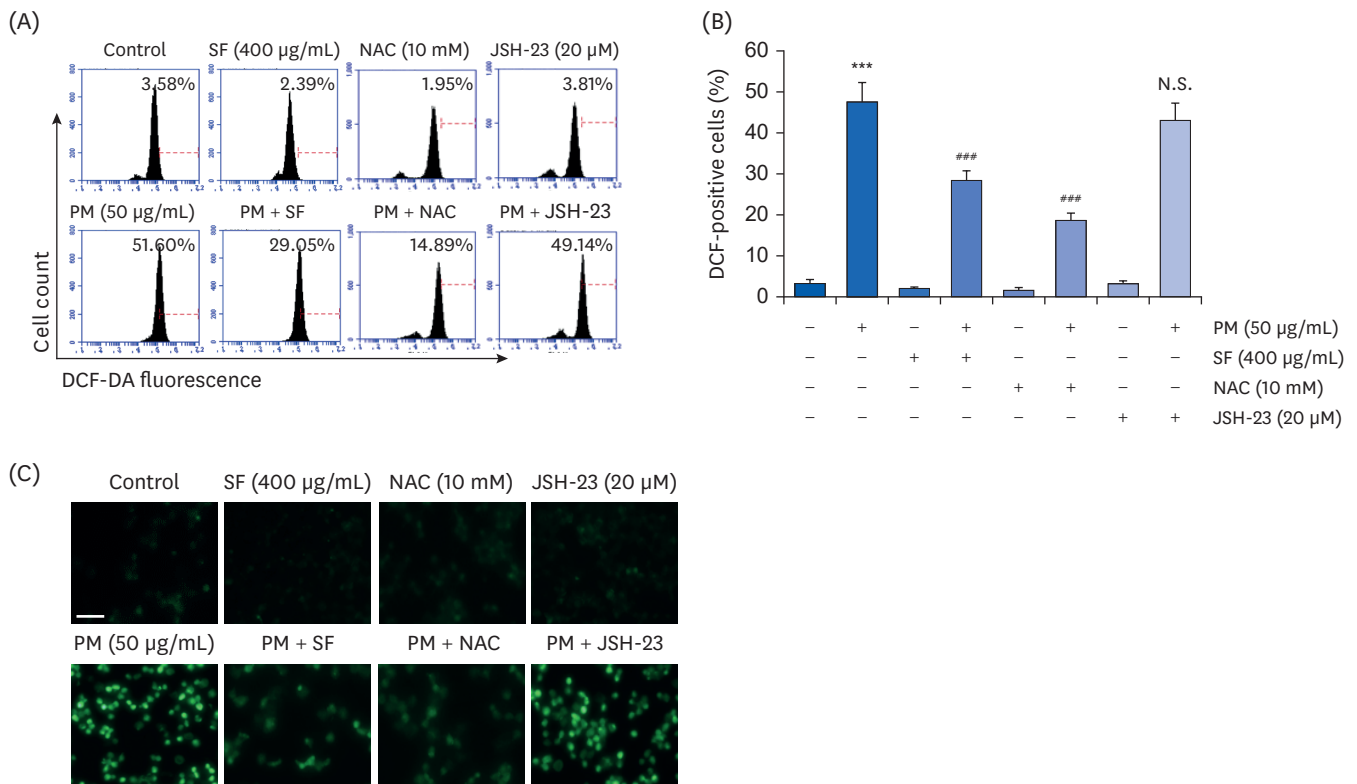


Fig. 4. Inhibition of ROS generation by SF in PM2.5-stimulated RAW 264.7 macrophages. Cells were pre-treated with 400 µg/mL SF, 10 mM NAC or 20 µM JSH-23 for 1 h and then treated with 50 µg/mL PM2.5 for 1 h. (A) The DCF-DA-stained cells were collected, and then DCF fluorescence was analyzed by flow cytometry. (B) Data are given as the mean ± SD of 3 independent experiments. (C) ROS generation was also detected by a fluorescence microscope and representative fluorescence micrographs depicting ROS generation are presented. Green fluorescence indicates the intensity of ROS generation (scale bar = 200 µM). ROS, reactive oxygen species; SF, Schisandrae Fructus ethanol extract; NAC, N-acetyl cysteine; JSH-23, 4-methyl-N¹-(3-phenyl-propyl)-benzene-1,2-diamine; DCF-DA, 5,6-carboxy-2',7'-dichlorofluorescein diacetate; N.S., not significant; PM, particulate matter. ****P* < 0.001 vs. PM2.5-unstimulated cells; *****P* < 0.001 vs. PM2.5-stimulated cells.

DISCUSSION

In this study, to evaluate the anti-inflammatory efficacy of SF against PM2.5, we first investigated its effect on the production of NO and PGE₂, which are classified as pro-inflammatory mediators [35-38]. Among them, NO, which is synthesized from L-arginine by NO synthase, plays a critical role in normal physiological conditions such as vasodilation, neurotransmission, and immune defense. However, excessive NO formation due to increased iNOS expression promotes the inflammatory response and increases oxidative stress [37,38]. COX enzymes catalyze the conversion of arachidonic acid to prostaglandins, including PGE₂, a group of hormone-like substances that participate in various body functions [35,36]. However, excessive PGE₂ production, promoted by the increased activity of COX-2 following various inflammatory stimuli, plays an important role as an inflammatory mediator [37,38]. Our data indicated that the up-graduated secretion of NO and PGE₂ by PM2.5 in RAW 264.7 macrophages was progressively inhibited at increasing concentrations of SF, which was associated with inhibition of the expression of iNOS and COX-2 mRNA and protein. These data demonstrated that the anti-inflammatory effect of SF was due to the reduced expression of iNOS and COX-2, which are involved in NO and PGE₂ production.

During the inflammatory response, macrophages secrete multiple pro-inflammatory cytokines that are involved in various signaling pathways producing autocrine and/or

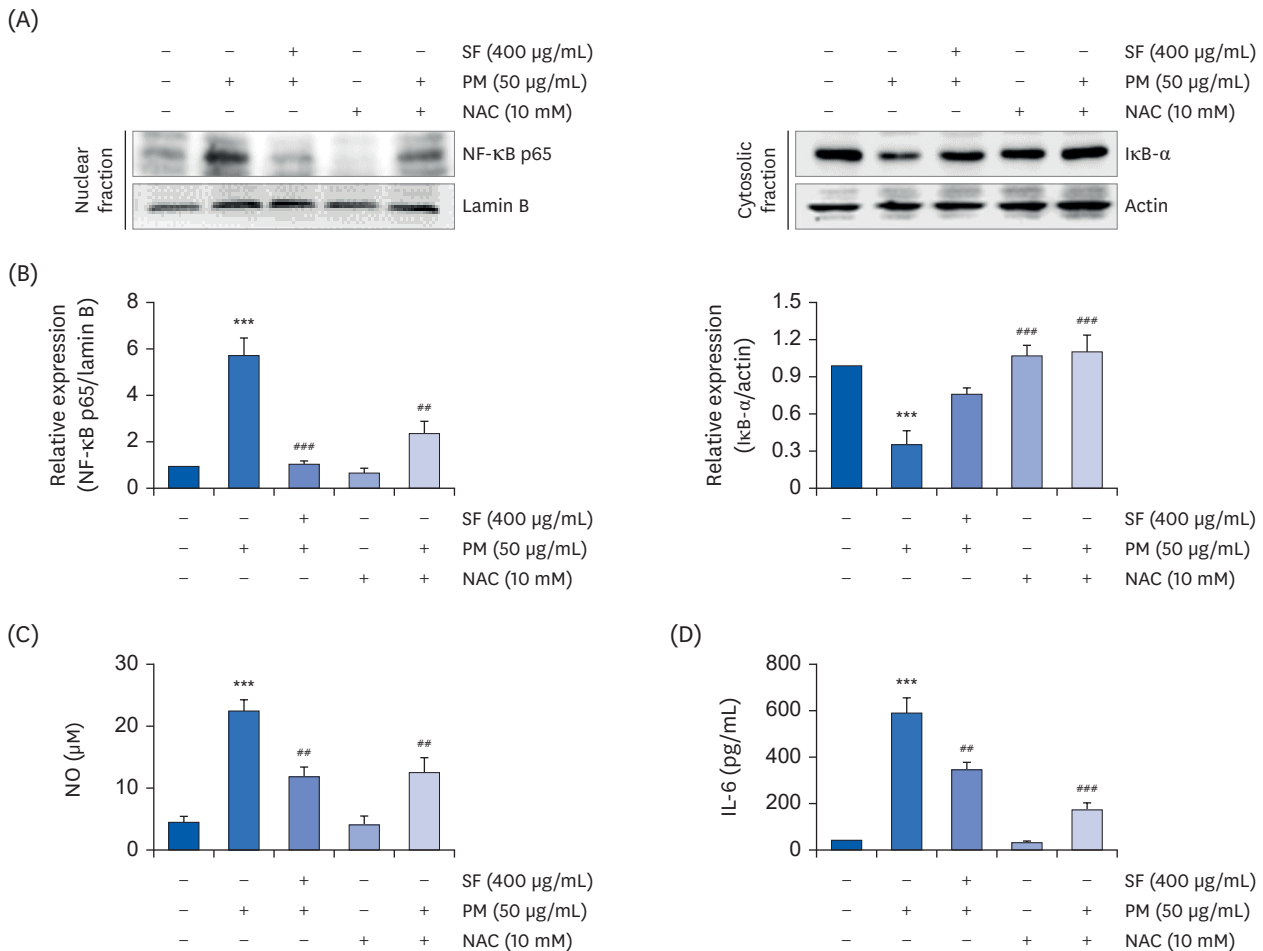


Fig. 5. Role of ROS on the inhibitory effect of SF on PM2.5-induced NF-κB activation and inflammatory response. Cells were pre-treated with 400 μg/mL SF or 10 mM NAC for 1 h and then treated with 50 μg/mL PM2.5 for 1 h (A, B) or 24 h (C, D). (A, B) Nuclear and cytosolic proteins were isolated, and the expression of NF-κB and IκB-α was investigated. Protein loading was confirmed by the analysis of lamin B or actin expression in each protein extract. (B) Bands were quantified using ImageJ and normalized to lamin B and actin, and the ratio was determined. The NO (C) and IL-6 (D) concentration in the culture medium was determined by the Griess reaction and IL-6 ELISA kit, respectively. The absorbance was measured using a microplate reader. (B-D) Data are expressed as the mean ± SD of 3 independent experiments.

ROS, reactive oxygen species; SF, Schisandrae Fructus ethanol extract; PM, particulate matter; NF-κB, nuclear factor-kappa B; NO, nitric oxide; IL, interleukin; ELISA, enzyme-linked immunosorbent assay.

****P* < 0.001 vs. PM-unstimulated cells; ***P* < 0.01 and *****P* < 0.001 vs. PM-stimulated cells.

paracrine effects [39-41]. All of these are essential components for the initiation and improvement of the inflammatory response, and their expression is also increased by the PM2.5 stimulation of macrophages [42-44]. Moreover, they can accelerate the inflammatory response by PM2.5 through activating or increasing the expression of pro-inflammatory mediators as well as other pro-inflammatory cytokines [45,46]. Therefore, the level of pro-inflammatory cytokines has been applied as an indicator to evaluate anti-inflammatory efficacy in macrophages. In the current study, we found that SF reduced the production of IL-6 and IL-1β in PM2.5-stimulated RAW 264.7 macrophages by suppressing their expression.

As noted in many studies, NF-κB plays a critical role in the control of inducible anti-inflammatory enzymes and cytokines in PM2.5-activated macrophages [8,44,47,48]. Typically, NF-κB forms a complex with the inhibitory subunit IκB-α and remains inactive in the cytoplasm. When IκB-α is phosphorylated and degraded through the upstream signaling systems by inflammatory stimuli, NF-κB migrates to the nucleus, triggering transcriptional

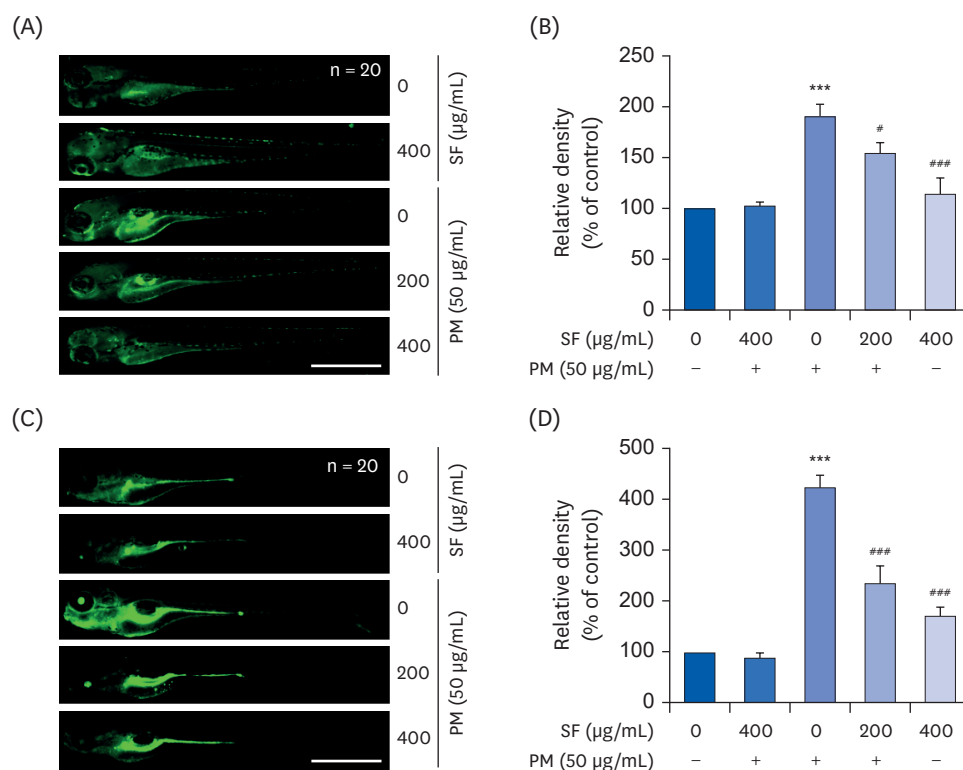


Fig. 6. Inhibition of PM2.5-induced NO and ROS generation by SF in zebrafish larvae. Zebrafish at 3 dpf were treated with 50 µg/mL PM2.5 and placed in E3 media containing the indicated concentrations of SF for 24 h. The larvae were incubated with 5 µM DAF-FM-DA (A, B) or 20 µM DCF-DA (C, D) for NO and ROS detection and visualized using the CELENA® S Digital Imaging System (scale bar = 1,000 µm). (B, D) Relative fluorescence intensities were calculated and expressed compared to the untreated control. Each value indicates the mean ± SD of 3 independent experiments. Significant differences among the groups were determined. PM, particulate matter; NO, nitric oxide; ROS, reactive oxygen species; SF, Schisandrae Fructus ethanol extract; dpf, days post-fertilized; DAF-FM-DA, 4-amino-5-methylamino-2',7'-difluorofluorescein diacetate; DCF-DA, 5,6-carboxy-2',7'-dichlorofluorescein diacetate.

*** $P < 0.001$ vs. PM2.5-unstimulated larvae; # $P < 0.05$ and *** $P < 0.001$ vs. PM2.5-stimulated larvae.

activation of inflammation-inducing genes and catabolic enzymes [49,50]. Therefore, the efficacy of SF on PM2.5-induced NF-κB activation was further evaluated because blocking the activity of NF-κB could be effective in treating inflammation. The current results showed that the translocation of NF-κB from the cytoplasm into the nucleus, and the degradation of IκB-α were increased in PM2.5-treated RAW 264.7 cells, but SF effectively blocked the nuclear translocation of NF-κB and the degradation of IκB-α. Therefore, the inhibitory effect of SF on the increased expression of pro-inflammatory enzymes and cytokines in PM2.5-treated RAW 264.7 macrophages is due to blocking of the nuclear translocation of NF-κB, and these results are in good agreement with the anti-inflammatory mechanisms of several natural compounds found in PM2.5-stimulated macrophages [48,51].

On the other hand, endogenous free radicals like ROS play an important role in host defense. However, excess ROS can cause oxidative damage to cellular macromolecules, and has been shown to play a key role in initiating and promoting inflammation-related diseases by upregulating the production of inflammatory mediators and cytokines. ROS also contribute to the activation of macrophages, and ROS generation is enhanced in overactive macrophages [52,53]. According to our results, SF strongly inhibited PM2.5-induced ROS formation in RAW 264.7 macrophages, similar to the action of a scavenger of oxidative stress

NAC. We subsequently examined the role of NF- κ B in the inflammatory response caused by PM2.5 using JSH-23, which inhibits NF- κ B transcriptional activity. In our results, JSH-23 showed a slight ROS inhibitory effect in PM2.5-treated cells compared to the conditions in the presence of SF or NAC, but was not significant. However, when the production of ROS was artificially blocked by the pretreatment of NAC, the nuclear accumulation of NF- κ B p65 and the degradation of I κ B by PM2.5 were remarkably suppressed, which was associated with inhibition of the anti-inflammatory reaction. Collectively, these findings suggest that SF exerts an anti-inflammatory effect in PM2.5-stimulated RAW 264.7 macrophages by down-regulating the activation of the ROS-dependent NF- κ B signaling pathway. Although the antioxidant potential of Schisandrae Fructus has been reported in several previous studies [24,26,52], the results of this study support the use of SF as an antioxidant for the management of oxidative stress associated with inflammatory responses by PM. Recently, zebrafish (*Danio rerio*), which have great advantages as an *in vivo* animal model, is widely used as a powerful vertebrate animal model for the study of human diseases [53,54]. In particular, since PM-stimulated zebrafish exhibit inflammatory and oxidative reactions similar to those of mammals, and is recognized as an optimal *in vivo* model for evaluating anti-inflammatory and antioxidant efficacy of various drugs [55-59]. Since *in vivo* experiments can provide a better understanding of efficacy assessment at the organism level, the anti-inflammatory and antioxidant potential of SF identified in macrophages was further confirmed in the zebrafish model. The results of this study showed the ability of SF to inhibit inflammatory and oxidative reactions in the PM2.5-treated zebrafish larvae model by reducing NO and ROS generation. Although these results support our *in vitro* results, additional mechanistic studies are needed to interpret the mechanisms related to the anti-inflammatory and antioxidant efficacy of SF in *in vivo* model. Furthermore, it is necessary to identify the active ingredients contained in SF that modulates the anti-inflammatory and/or antioxidant responses in RAW 264.7 macrophages stimulated with PM2.5.

In summary, in the present study, we demonstrated that SF markedly reversed the production of pro-inflammatory mediators and cytokines in PM2.5-treated RAW 264.7 macrophages. In addition, SF significantly attenuated PM2.5-induced ROS production, and enhanced the inactivation of the NF- κ B signaling pathway. Furthermore, the anti-inflammatory and antioxidant activities of SF were also confirmed in an *in vivo* zebrafish model. Therefore, our results suggest that SF or its constituents may minimize the severity of oxidative stress and inflammation caused by PM2.5. However, further studies are needed to determine the role of other cellular signaling pathways that may be involved in the anti-inflammatory activity of SF other than the NF- κ B signaling pathway, and to determine the direct relationship with NF- κ B signaling.

REFERENCES

1. Loxham M, Nieuwenhuijsen MJ. Health effects of particulate matter air pollution in underground railway systems - a critical review of the evidence. Part Fibre Toxicol 2019;16:12.
[PUBMED](#) | [CROSSREF](#)
2. Almetwally AA, Bin-Jumah M, Allam AA. Ambient air pollution and its influence on human health and welfare: an overview. Environ Sci Pollut Res Int 2020;27:24815-30.
[PUBMED](#) | [CROSSREF](#)
3. Lynch HN, Loftus CT, Cohen JM, Kerper LE, Kennedy EM, Goodman JE. Weight-of-evidence evaluation of associations between particulate matter exposure and biomarkers of lung cancer. Regul Toxicol Pharmacol 2016;82:53-93.
[PUBMED](#) | [CROSSREF](#)

4. Wu JZ, Ge DD, Zhou LF, Hou LY, Zhou Y, Li QY. Effects of particulate matter on allergic respiratory diseases. *Chronic Dis Transl Med* 2018;4:95-102.
[PUBMED](#) | [CROSSREF](#)
5. Combes A, Franchineau G. Fine particle environmental pollution and cardiovascular diseases. *Metabolism* 2019;100S:153944.
[PUBMED](#) | [CROSSREF](#)
6. Liu B, Wu J, Zhang J, Wang L, Yang J, Liang D, Dai Q, Bi X, Feng Y, Zhang Y, Zhang Q. Characterization and source apportionment of PM_{2.5} based on error estimation from EPA PMF 5.0 model at a medium city in China. *Environ Pollut* 2017;222:10-22.
[PUBMED](#) | [CROSSREF](#)
7. Yang Y, Ruan Z, Wang X, Yang Y, Mason TG, Lin H, Tian L. Short-term and long-term exposures to fine particulate matter constituents and health: a systematic review and meta-analysis. *Environ Pollut* 2019;247:874-82.
[PUBMED](#) | [CROSSREF](#)
8. He M, Ichinose T, Yoshida S, Ito T, He C, Yoshida Y, Arashidani K, Takano H, Sun G, Shibamoto T. PM_{2.5}-induced lung inflammation in mice: differences of inflammatory response in macrophages and type II alveolar cells. *J Appl Toxicol* 2017;37:1203-18.
[PUBMED](#) | [CROSSREF](#)
9. Tang Q, Huang K, Liu J, Wu S, Shen D, Dai P, Li C. Fine particulate matter from pig house induced immune response by activating TLR4/MAPK/NF-κB pathway and NLRP3 inflammasome in alveolar macrophages. *Chemosphere* 2019;236:124373.
[PUBMED](#) | [CROSSREF](#)
10. Shukla A, Timblin C, BeruBe K, Gordon T, McKinney W, Driscoll K, Vacek P, Mossman BT. Inhaled particulate matter causes expression of nuclear factor (NF)-kappaB-related genes and oxidant-dependent NF-kappaB activation *in vitro*. *Am J Respir Cell Mol Biol* 2000;23:182-7.
[PUBMED](#) | [CROSSREF](#)
11. Jeong S, Park SA, Park I, Kim P, Cho NH, Hyun JW, Hyun YM. PM_{2.5} Exposure in the respiratory system induces distinct inflammatory signaling in the lung and the liver of mice. *J Immunol Res* 2019;2019:3486841.
[PUBMED](#) | [CROSSREF](#)
12. Wyatt LH, Devlin RB, Rappold AG, Case MW, Diaz-Sanchez D. Low levels of fine particulate matter increase vascular damage and reduce pulmonary function in young healthy adults. *Part Fibre Toxicol* 2020;17:58.
[PUBMED](#) | [CROSSREF](#)
13. Piao MJ, Ahn MJ, Kang KA, Ryu YS, Hyun YJ, Shilnikova K, Zhen AX, Jeong JW, Choi YH, Kang HK, Koh YS, Hyun JW. Particulate matter 2.5 damages skin cells by inducing oxidative stress, subcellular organelle dysfunction, and apoptosis. *Arch Toxicol* 2018;92:2077-91.
[PUBMED](#) | [CROSSREF](#)
14. Lee H, Hwang-Bo H, Ji SY, Kim MY, Kim SY, Park C, Hong SH, Kim GY, Song KS, Hyun JW, Choi YH. Diesel particulate matter_{2.5} promotes epithelial-mesenchymal transition of human retinal pigment epithelial cells via generation of reactive oxygen species. *Environ Pollut* 2020;262:114301.
[PUBMED](#) | [CROSSREF](#)
15. Wei H, Yuan W, Yu H, Geng H. Cytotoxicity induced by fine particulate matter (PM_{2.5}) *via* mitochondria-mediated apoptosis pathway in rat alveolar macrophages. *Environ Sci Pollut Res Int* 2021;21:111.
[PUBMED](#) | [CROSSREF](#)
16. Rao X, Zhong J, Brook RD, Rajagopalan S. Effect of particulate matter air pollution on cardiovascular oxidative stress pathways. *Antioxid Redox Signal* 2018;28:797-818.
[PUBMED](#) | [CROSSREF](#)
17. Øvrevik J. Oxidative potential versus biological effects: a review on the relevance of cell-free/abiotic assays as predictors of toxicity from airborne particulate matter. *Int J Mol Sci* 2019;20:4772.
[PUBMED](#) | [CROSSREF](#)
18. Guan L, Geng X, Stone C, Cosky EE, Ji Y, Du H, Zhang K, Sun Q, Ding Y. PM_{2.5} exposure induces systemic inflammation and oxidative stress in an intracranial atherosclerosis rat model. *Environ Toxicol* 2019;34:530-8.
[PUBMED](#) | [CROSSREF](#)
19. Panossian A, Wikman G. Pharmacology of *Schisandra chinensis* Bail.: an overview of Russian research and uses in medicine. *J Ethnopharmacol* 2008;118:183-212.
[PUBMED](#) | [CROSSREF](#)

20. Zhang M, Xu L, Yang H. *Schisandra chinensis* Fructus and its active ingredients as promising resources for the treatment of neurological diseases. *Int J Mol Sci* 2018;19:1970.
[PUBMED](#) | [CROSSREF](#)
21. Chun JN, Cho M, So I, Jeon JH. The protective effects of *Schisandra chinensis* fruit extract and its lignans against cardiovascular disease: a review of the molecular mechanisms. *Fitoterapia* 2014;97:224-33.
[PUBMED](#) | [CROSSREF](#)
22. Nowak A, Zaklos-Szyda M, Blasiak J, Nowak A, Zhang Z, Zhang B. Potential of *Schisandra chinensis* (Turcz.) Baill. in human health and nutrition: a review of current knowledge and therapeutic perspectives. *Nutrients* 2019;11:333.
[PUBMED](#) | [CROSSREF](#)
23. Song FJ, Zeng KW, Chen JF, Li Y, Song XM, Tu PF, Wang XM. Extract of Fructus *Schisandrae chinensis* inhibits neuroinflammation mediator production from microglia *via* NF-kappa B and MAPK pathways. *Chin J Integr Med* 2019;25:131-8.
[PUBMED](#) | [CROSSREF](#)
24. Jeong JW, Lee HH, Choi EO, Lee KW, Kim KY, Kim SG, Hong SH, Kim GY, Park C, Kim HK, Choi YW, Choi YH. Schisandrae Fructus inhibits IL-1beta-induced matrix metalloproteinases and inflammatory mediators production in SW1353 human chondrocytes by suppressing NF-kappaB and MAPK activation. *Drug Dev Res* 2015;76:474-83.
[PUBMED](#) | [CROSSREF](#)
25. Dilshara MG, Jayasooriya RG, Kang CH, Lee S, Park SR, Jeong JW, Choi YH, Seo YT, Jang YP, Kim GY. Downregulation of pro-inflammatory mediators by a water extract of *Schisandra chinensis* (Turcz.) Baill fruit in lipopolysaccharide-stimulated RAW 264.7 macrophage cells. *Environ Toxicol Pharmacol* 2013;36:256-64.
[PUBMED](#) | [CROSSREF](#)
26. Kang JS, Han MH, Kim GY, Kim CM, Kim BW, Hwang HJ, Hyun Y. Nrf2-mediated HO-1 induction contributes to antioxidant capacity of a Schisandrae Fructus ethanol extract in C2C12 myoblasts. *Nutrients* 2014;6:5667-78.
[PUBMED](#) | [CROSSREF](#)
27. Karna KK, Choi BR, Kim MJ, Kim HK, Park JK. The effect of *Schisandra chinensis* Baillon on cross-talk between oxidative stress, endoplasmic reticulum stress, and mitochondrial signaling pathway in testes of varicocele-induced SD rat. *Int J Mol Sci* 2019;20:5785.
[PUBMED](#) | [CROSSREF](#)
28. Jeong JW, Kim J, Choi EO, Kwon DH, Kong GM, Choi IW, Kim BH, Kim GY, Lee KW, Kim KY, Kim SG, Choi YW, Hong SH, Park C, Choi YH. Schisandrae Fructus ethanol extract ameliorates inflammatory responses and articular cartilage damage in monosodium iodoacetate-induced osteoarthritis in rats. *EXCLI J* 2017;16:265-77.
[PUBMED](#) | [CROSSREF](#)
29. Choi YH. Trans-cinnamaldehyde protects C2C12 myoblasts from DNA damage, mitochondrial dysfunction and apoptosis caused by oxidative stress through inhibiting ROS production. *Genes Genomics* 2021;43:303-12.
[PUBMED](#) | [CROSSREF](#)
30. Chae BS. Effect of low-dose corticosterone pretreatment on the production of inflammatory mediators in super-low-dose LPS-primed immune cells. *Toxicol Res* 2021;37:47-57.
[PUBMED](#) | [CROSSREF](#)
31. Park S, Kim M, Hong Y, Lee H, Tran Q, Kim C, Kwon SH, Park J, Park J, Kim SH. Myristoylated TMEM39AS41, a cell-permeable peptide, causes lung cancer cell death. *Toxicol Res* 2020;36:123-30.
[PUBMED](#) | [CROSSREF](#)
32. Park JW, Lee SJ, Kim JE, Kang MJ, Bae SJ, Choi YJ, Gong JE, Kim KS, Jung YS, Cho JY, Choi YS, Hwang DY, Song HK. Comparison of response to LPS-induced sepsis in three DBA/2 stocks derived from different sources. *Lab Anim Res* 2021;37:2.
[PUBMED](#) | [CROSSREF](#)
33. Hwangbo H, Kim SY, Lee H, Park SH, Hong SH, Park C, Kim GY, Leem SH, Hyun JW, Cheong J, Choi YH. Auranofin enhances sulforaphane-mediated apoptosis in hepatocellular carcinoma Hep3B cells through inactivation of the PI3K/Akt signaling pathway. *Biomol Ther* 2020;28:443-55.
[PUBMED](#) | [CROSSREF](#)
34. Jeong JW, Cha HJ, Han MH, Hwang SJ, Lee DS, Yoo JS, Choi IW, Kim S, Kim HS, Kim GY, Hong SH, Park C, Lee HJ, Choi YH. Spermidine protects against oxidative stress in inflammation models using macrophages and zebrafish. *Biomol Ther* 2018;26:146-56.
[PUBMED](#) | [CROSSREF](#)
35. Soufli I, Toumi R, Rifa H, Touil-Boukoffa C. Overview of cytokines and nitric oxide involvement in immunopathogenesis of inflammatory bowel diseases. *World J Gastrointest Pharmacol Ther* 2016;7:353-60.
[PUBMED](#) | [CROSSREF](#)

36. Aleem D, Tohid H. Pro-inflammatory cytokines, biomarkers, genetics and the immune system: a mechanistic approach of depression and psoriasis. *Rev Colomb Psiquiatr* 2018;47:177-86.
[PUBMED](#) | [CROSSREF](#)
37. Saini R, Singh S. Inducible nitric oxide synthase: an asset to neutrophils. *J Leukoc Biol* 2019;105:49-61.
[PUBMED](#) | [CROSSREF](#)
38. Yao C, Narumiya S. Prostaglandin-cytokine crosstalk in chronic inflammation. *Br J Pharmacol* 2019;176:337-54.
[PUBMED](#) | [CROSSREF](#)
39. Wang T, He C, Yu X. Pro-inflammatory cytokines: new potential therapeutic targets for obesity-related bone disorders. *Curr Drug Targets* 2017;18:1664-75.
[PUBMED](#) | [CROSSREF](#)
40. Hu F, Lou N, Jiao J, Guo F, Xiang H, Shang D. Macrophages in pancreatitis: Mechanisms and therapeutic potential. *Biomed Pharmacother* 2020;131:110693.
[PUBMED](#) | [CROSSREF](#)
41. Zhang H, Cai D, Bai X. Macrophages regulate the progression of osteoarthritis. *Osteoarthritis Cartilage* 2020;28:555-61.
[PUBMED](#) | [CROSSREF](#)
42. Jalava PI, Salonen RO, Pennanen AS, Happonen MS, Penttinen P, Hälinen AI, Sillanpää M, Hillamo R, Hirvonen MR. Effects of solubility of urban air fine and coarse particles on cytotoxic and inflammatory responses in RAW 264.7 macrophage cell line. *Toxicol Appl Pharmacol* 2008;229:146-60.
[PUBMED](#) | [CROSSREF](#)
43. Bekki K, Ito T, Yoshida Y, He C, Arashidani K, He M, Sun G, Zeng Y, Sone H, Kunugita N, Ichinose T. PM2.5 collected in China causes inflammatory and oxidative stress responses in macrophages through the multiple pathways. *Environ Toxicol Pharmacol* 2016;45:362-9.
[PUBMED](#) | [CROSSREF](#)
44. Zhu J, Zhao Y, Gao Y, Li C, Zhou L, Qi W, Zhang Y, Ye L. Effects of different components of PM_{2.5} on the expression levels of NF-kappaB family gene mRNA and inflammatory molecules in human macrophage. *Int J Environ Res Public Health* 2019;16:1408.
[PUBMED](#) | [CROSSREF](#)
45. Yin J, Xia W, Li Y, Guo C, Zhang Y, Huang S, Jia Z, Zhang A. COX-2 mediates PM2.5-induced apoptosis and inflammation in vascular endothelial cells. *Am J Transl Res* 2017;9:3967-76.
[PUBMED](#)
46. Beck-Speier I, Kreyling WG, Maier KL, Dayal N, Schladweiler MC, Mayer P, Semmler-Behnke M, Kodavanti UP. Soluble iron modulates iron oxide particle-induced inflammatory responses *via* prostaglandin E₂ synthesis: *in vitro* and *in vivo* studies. *Part Fibre Toxicol* 2009;6:34.
[PUBMED](#) | [CROSSREF](#)
47. Migliaccio CT, Kobos E, King QO, Porter V, Jessop F, Ward T. Adverse effects of wood smoke PM_{2.5} exposure on macrophage functions. *Inhal Toxicol* 2013;25:67-76.
[PUBMED](#) | [CROSSREF](#)
48. Li W, Cai ZN, Mehmood S, Liang LL, Liu Y, Zhang HY, Chen Y, Lu YM. Anti-inflammatory effects of *Morchella esculenta* polysaccharide and its derivatives in fine particulate matter-treated NR8383 cells. *Int J Biol Macromol* 2019;129:904-15.
[PUBMED](#) | [CROSSREF](#)
49. Rigoglou S, Papavassiliou AG. The NF-κB signalling pathway in osteoarthritis. *Int J Biochem Cell Biol* 2013;45:2580-4.
[PUBMED](#) | [CROSSREF](#)
50. Schuliga M. NF-kappaB signaling in chronic inflammatory airway disease. *Biomolecules* 2015;5:1266-83.
[PUBMED](#) | [CROSSREF](#)
51. Shi Y, Batibawa JW, Maiga M, Sun B, Li Y, Duan J, Sun Z. Identification and validation of metformin protects against PM_{2.5}-induced macrophages cytotoxicity by targeting toll like receptor pathway. *Chemosphere* 2020;251:126526.
[PUBMED](#) | [CROSSREF](#)
52. Liu Z, Ren Z, Zhang J, Chuang CC, Kandaswamy E, Zhou T, Zuo L. Role of ROS and nutritional antioxidants in human diseases. *Front Physiol* 2018;9:477.
[PUBMED](#) | [CROSSREF](#)
53. Mills EL, O'Neill LA. Reprogramming mitochondrial metabolism in macrophages as an anti-inflammatory signal. *Eur J Immunol* 2016;46:13-21.
[PUBMED](#) | [CROSSREF](#)

54. Bailone RL, Fukushima HC, Ventura Fernandes BH, De Aguiar LK, Corrêa T, Janke H, Grejo Setti P, Roça RO, Borra RC. Zebrafish as an alternative animal model in human and animal vaccination research. *Lab Anim Res* 2020;36:13.
[PUBMED](#) | [CROSSREF](#)
55. Ren F, Huang Y, Tao Y, Ji C, Aniagu S, Jiang Y, Chen T. Resveratrol protects against PM2.5-induced heart defects in zebrafish embryos as an antioxidant rather than as an AHR antagonist. *Toxicol Appl Pharmacol* 2020;398:115029.
[PUBMED](#) | [CROSSREF](#)
56. Zhang Y, Li S, Li J, Han L, He Q, Wang R, Wang X, Liu K. Developmental toxicity induced by PM2.5 through endoplasmic reticulum stress and autophagy pathway in zebrafish embryos. *Chemosphere* 2018;197:611-21.
[PUBMED](#) | [CROSSREF](#)
57. Dai YL, Jiang YF, Lu YA, Yu JB, Kang MC, Jeon YJ. Fucoxanthin-rich fraction from *Sargassum fusiformis* alleviates particulate matter-induced inflammation *in vitro* and *in vivo*. *Toxicol Rep* 2021;8:349-58.
[PUBMED](#) | [CROSSREF](#)
58. de Abreu MS, Giacomini AC, Genario R, Dos Santos BE, da Rosa LG, Demin KA, Wappler-Guzzetta EA, Kalueff AV. Neuropharmacology, pharmacogenetics and pharmacogenomics of aggression: the zebrafish model. *Pharmacol Res* 2019;141:602-8.
[PUBMED](#) | [CROSSREF](#)
59. Duan J, Yu Y, Li Y, Wang Y, Sun Z. Inflammatory response and blood hypercoagulable state induced by low level co-exposure with silica nanoparticles and benzo[a]pyrene in zebrafish (*Danio rerio*) embryos. *Chemosphere* 2016;151:152-62.
[PUBMED](#) | [CROSSREF](#)